

**A 2D Fluid Model of the DC Planar
Magnetron Cathode**

Manuel Garcia

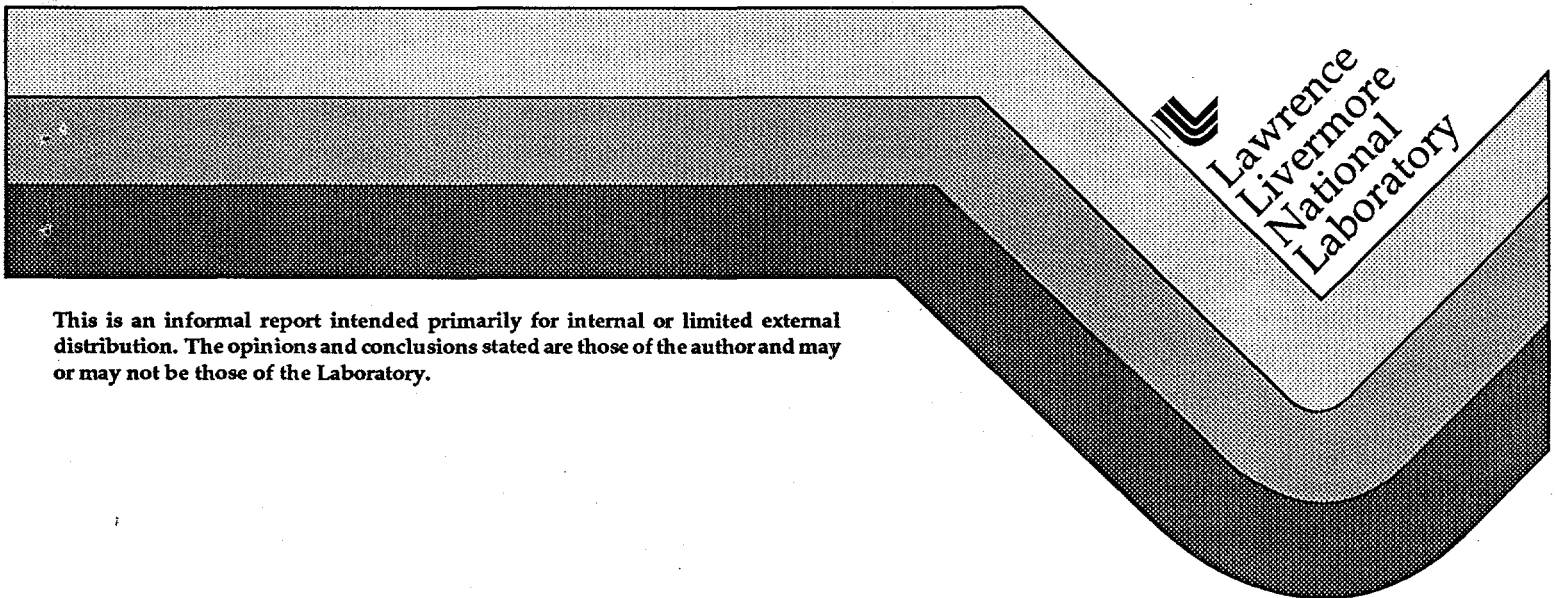
RECEIVED

JUN 27 1996

OSTI

MASTER

October 3, 1995



This is an informal report intended primarily for internal or limited external distribution. The opinions and conclusions stated are those of the author and may or may not be those of the Laboratory.

DISCLAIMER

This report was prepared as an account of work sponsored by an agency of the United States Government. Neither the United States Government nor any agency thereof, nor any of their employees, makes any warranty, express or implied, or assumes any legal liability or responsibility for the accuracy, completeness, or usefulness of any information, apparatus, product, or process disclosed, or represents that its use would not infringe privately owned rights. Reference herein to any specific commercial product, process, or service by trade name, trademark, manufacturer, or otherwise does not necessarily constitute or imply its endorsement, recommendation, or favoring by the United States Government or any agency thereof. The views and opinions of authors expressed herein do not necessarily state or reflect those of the United States Government or any agency thereof.

DISCLAIMER

**Portions of this document may be illegible
in electronic image products. Images are
produced from the best available original
document.**

A 2D Fluid Model of the DC Planar Magnetron Cathode

Manuel Garcia
3 October 1995

Lawrence Livermore National Laboratory, L-490, P.O. Box 808, Livermore CA 94550
garcia22@llnl.gov, (510) 422-6017, FAX: (510) 422-7748

This model finds the plasma density distribution, $n(x,y)$, and the positive electrical potential, ϕ_{∞} , between the surface of a planar magnetron cathode and a distant, uniform plasma. The intended application is for parameter studies of gas discharges in the range of 1-100 mTorr, which are often used as sputtering sources. The primary results are formulas which show how the spatial variation of the magnetic field, $B(x,y)$, shapes the plasma density and influences the potential, as well as determining the magnitude of the magnetron current parallel to the cathode surface.

Introduction

Planar magnetron cathodes have arching magnetic field lines which concentrate plasma density near the electrode surface. This enhances the ion bombardment of the surface and the yield of sputtered atoms. Because of the current density concentration at these cathodes they can be used to operate gas discharge devices at lower voltage for a given current. An essential feature is that the vector product of the perpendicular electric field, E_y , with the parallel component of the magnetic field, B_x , forms a closed track with a circulating current along the cathode surface.^{1,2,3,4,5,6,7,8} Figure 1 shows a cross section of a pair of antiparallel linear planar magnetron tracks, and the coordinate system convention used here.

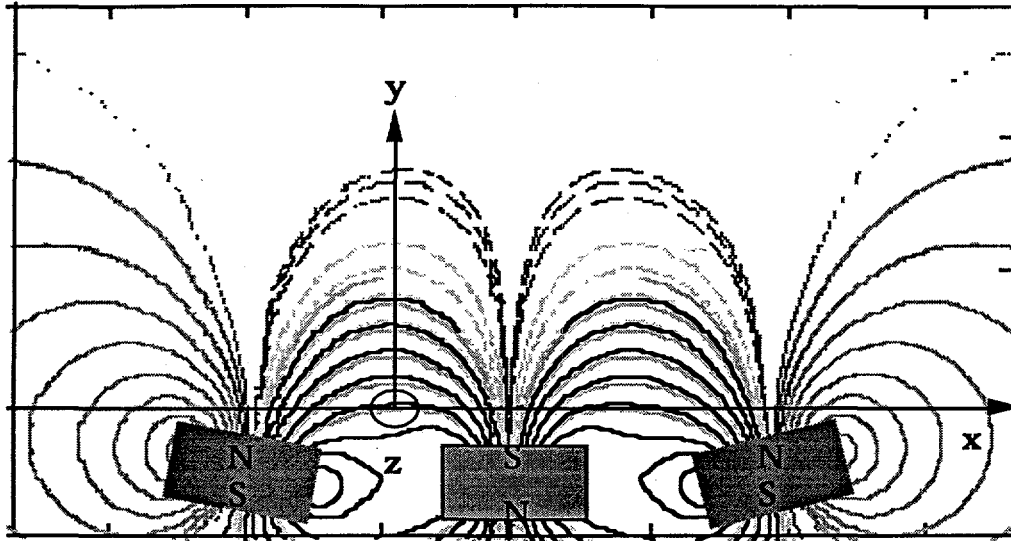


Figure 1: Pair of antiparallel linear magnetron tracks, cathode surface at $y=0$

This model utilizes the fluid equations for both a positive ion and electron species, and it relies on the assumption that only electron motion is affected by the magnetic field. Figure 2 is a schematic of a single linear magnetron track. It shows the spatial relationship between the electric and magnetic fields, the plasma density, the conduction current carried by ions flowing in the $-y$ direction, and the magnetron current produced by electron drift along z .

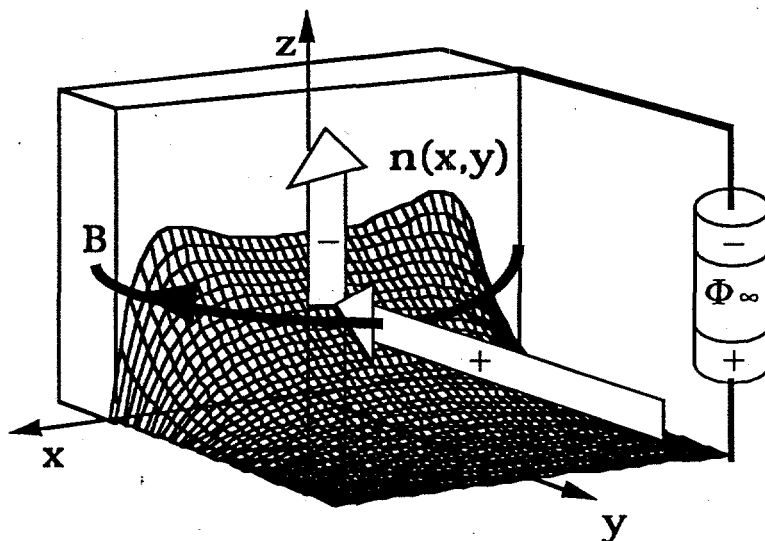


Figure 2: Schematic of linear magnetron cathode track

The derivation of this model will be presented in detail, and then numerical examples will be shown.

Governing Equations

A two component fluid model for electrons and positive ions in the presence of a static, non-reactive background gas is used. Four basic assumptions are: ions are unaffected by \mathbf{B} , electrons cling to lines of \mathbf{B} and have limited mobility, the magnetic field is unaffected by plasma density and is of the form $\mathbf{B}(x,y) = B_x(x,y) \mathbf{i} + B_y(x,y) \mathbf{j}$, there is no variation in z for any quantity. The equations of mass and momentum conservation are:

$$\frac{\partial \rho_\alpha}{\partial t} + \nabla \cdot \rho_\alpha \mathbf{v}_\alpha = m_\alpha S_\alpha \quad (1)$$

$$\frac{\partial \mathbf{v}_\alpha}{\partial t} + \mathbf{v}_\alpha \cdot \nabla \mathbf{v}_\alpha = \frac{q_\alpha}{m_\alpha} (\mathbf{E} + \mathbf{v}_\alpha \times \mathbf{B}) - \frac{\nabla p_\alpha}{\rho_\alpha} - \nu_{\alpha N} (\mathbf{v}_\alpha - \mathbf{U}_N) \quad (2)$$

for species labeled by subscript α , with mass density ρ , velocity \mathbf{v} , particle mass m , production rate per unit mass S , charge q , pressure p , collision frequency with the background gas ν , and for $\mathbf{U}_N = 0$ as the average velocity of the background gas. \mathbf{E} is the electric field.

The energy equations to be used here are for an adiabatic system with each species at its own constant temperature. This will be discussed in detail in a later section. The equations of state assume each species is an ideal gas:

$$\begin{aligned} \rho_\alpha &= n_\alpha m_\alpha \\ p_\alpha &= n_\alpha k T_\alpha \\ p_\alpha / \rho_\alpha &= \text{constant} \\ \nabla p_\alpha &= (U_\alpha^2 \equiv \gamma p_\alpha / \rho_\alpha) \nabla \rho_\alpha \\ U_\alpha^2 &= \gamma k T_\alpha / m_\alpha \end{aligned} \quad (3)$$

where n is the number density, T is the temperature, γ is the ratio of specific heats, and $k = 1.38054 \times 10^{-23}$ Joule/°K, the Boltzmann constant.

The electromagnetic equations are:

$$\text{curl } \mathbf{B} = \mu_0 \mathbf{j} + \frac{1}{c^2} \frac{\partial \mathbf{E}}{\partial t} \quad (-> 0, \text{ here}) \quad (4)$$

$$\nabla \cdot \mathbf{E} = \frac{\rho_c}{\epsilon_0} \quad (-> 0, \text{ here}) \quad (5)$$

$$\frac{\partial \rho_c}{\partial t} + \nabla \cdot \mathbf{j} = 0 \quad (6)$$

where \mathbf{j} is the current density, and ρ_c is the charge density.

Defined Quantities

The following definitions are used:

$\Gamma_\alpha = n_\alpha \mathbf{v}_\alpha$	species flux vectors	
$\mathbf{j}_\alpha = q_\alpha \Gamma_\alpha$	species current densities	
$\mathbf{j} = \mathbf{j}_+ + \mathbf{j}_e = e(\Gamma_+ - \Gamma_e)$	net current density	
$\rho_c = e(n_+ - n_e)$	charge density	
$D_\alpha = kT_\alpha / m_\alpha v_{\alpha N}$	diffusion coefficients	
$\mu_\alpha = q_\alpha / m_\alpha v_{\alpha N} $	mobility coefficients	
$D_\alpha / \mu_\alpha = kT_\alpha / q_\alpha $	characteristic energies (eV)	(7)

Steady State Equations

The governing equations in steady state are:

$$\nabla \cdot \Gamma_\alpha = S_\alpha \quad (8)$$

$$\frac{\mathbf{v}_\alpha \cdot \nabla \mathbf{v}_\alpha}{v_{\alpha N}} = \frac{q_\alpha}{|q_\alpha|} \mu_\alpha (\mathbf{E} + \mathbf{v}_\alpha \times \mathbf{B}) - \frac{D_\alpha \nabla n_\alpha}{n_\alpha} - \mathbf{v}_\alpha \quad (9)$$

$$\text{curl } \mathbf{B} = \mu_0 \mathbf{j} \quad (10)$$

$$\nabla \cdot \mathbf{E} = e(n_+ - n_e)/\epsilon_0 \quad (11)$$

$$\nabla \cdot \mathbf{j} = 0 \quad (12)$$

Two Fluid Flux Equations

From the definition of Γ_α and momentum equation (9):

$$\Gamma_\alpha = n_\alpha \frac{q_\alpha}{|q_\alpha|} \mu_\alpha (\mathbf{E} + \mathbf{v}_\alpha \times \mathbf{B}) - D_\alpha \nabla n_\alpha - \frac{n_\alpha \mathbf{v}_\alpha \cdot \nabla \mathbf{v}_\alpha}{v_{\alpha N}} \quad (13)$$

while from continuity equation (8) and current conservation (12) $S_+ = S_e \equiv S$. For electrons and positive ions as assumed here:

$$\Gamma_e = -n_e \mu_e (\mathbf{E} + \mathbf{v}_e \times \mathbf{B}) - D_e \nabla n_e - \frac{n_e \mathbf{v}_e \cdot \nabla \mathbf{v}_e}{v_{eN}} \quad (14)$$

$$\Gamma_+ = n_+ \mu_+ \mathbf{E} - D_+ \nabla n_+ - \frac{n_+ \mathbf{v}_+ \cdot \nabla \mathbf{v}_+}{v_{+N}} \quad (15)$$

$$\nabla \cdot \Gamma_+ = \nabla \cdot \Gamma_e = S \quad (16)$$

Component Fluxes

Component fluxes in a Cartesian coordinate system centered on a magnetron track as shown in Figures 1 and 2 are defined as follows:

$$\Gamma_\alpha = \Gamma_{\alpha x} \mathbf{i} + \Gamma_{\alpha y} \mathbf{j} + \Gamma_{\alpha z} \mathbf{k}$$

$$\Gamma_{ex} = -n_e \mu_e E_x + \mu_e n_e v_{ez} B_y - D_e \frac{\partial n_e}{\partial x} - \frac{n_e}{v_{eN}} (v_{ex} \frac{\partial v_{ex}}{\partial x} + v_{ey} \frac{\partial v_{ex}}{\partial y}) \quad (17)$$

$$\Gamma_{ey} = -n_e \mu_e E_y - \mu_e n_e v_{ez} B_x - D_e \frac{\partial n_e}{\partial y} - \frac{n_e}{v_{eN}} (v_{ex} \frac{\partial v_{ey}}{\partial x} + v_{ey} \frac{\partial v_{ey}}{\partial y}) \quad (18)$$

$$\Gamma_{ez} = -\mu_e n_e (v_{ex} B_y - v_{ey} B_x) - \frac{n_e}{v_{eN}} (v_{ex} \frac{\partial v_{ez}}{\partial x} + v_{ey} \frac{\partial v_{ez}}{\partial y}) \quad (19)$$

$$\Gamma_{+x} = n_+ \mu_+ E_x - D_+ \frac{\partial n_+}{\partial x} - \frac{n_+}{v_{+N}} (v_{+x} \frac{\partial v_{+x}}{\partial x} + v_{+y} \frac{\partial v_{+x}}{\partial y}) \quad (20)$$

$$\Gamma_{+y} = n_+ \mu_+ E_y - D_+ \frac{\partial n_+}{\partial y} - \frac{n_+}{v_{+N}} (v_{+x} \frac{\partial v_{+y}}{\partial x} + v_{+y} \frac{\partial v_{+y}}{\partial y}) \quad (21)$$

and $\Gamma_{+z} = 0$, as v_{+z} and E_z are assumed zero.

Component Current Densities and Quasi-neutrality

The component current densities are found from flux equations (17) through (21) and the definitions:

$$j_x = e(\Gamma_{+x} - \Gamma_{ex}) \quad j_y = e(\Gamma_{+y} - \Gamma_{ey}) \quad j_z = -e\Gamma_{ez} \quad (22)$$

The plasma is assumed to have sufficient density that electrostatic sheaths are thin, and the spatial distribution of the two fluids coincide. This is the assumption of quasi-neutrality:

$$n_e \approx n_+ = n$$

The component current densities are then found to be:

$$\begin{aligned} \frac{j_x}{e} = & n(\mu_+ + \mu_e)E_x - n\mu_e v_{ez} B_y + (D_e - D_+) \frac{\partial n}{\partial x} + \\ & \frac{n}{v_{eN}} (v_{ex} \frac{\partial v_{ex}}{\partial x} + v_{ey} \frac{\partial v_{ex}}{\partial y}) - \frac{n}{v_{+N}} (v_{+x} \frac{\partial v_{+x}}{\partial x} + v_{+y} \frac{\partial v_{+x}}{\partial y}) \end{aligned} \quad (23)$$

$$\begin{aligned} \frac{j_y}{e} = & n(\mu_+ + \mu_e)E_y + n\mu_e v_{ez} B_x + (D_e - D_+) \frac{\partial n}{\partial y} + \\ & \frac{n}{v_{eN}} (v_{ex} \frac{\partial v_{ey}}{\partial x} + v_{ey} \frac{\partial v_{ey}}{\partial y}) - \frac{n}{v_{+N}} (v_{+x} \frac{\partial v_{+y}}{\partial x} + v_{+y} \frac{\partial v_{+y}}{\partial y}) \end{aligned} \quad (24)$$

$$\frac{j_z}{en} = \mu_e(v_{ex}B_y - v_{ey}B_x) + \frac{1}{v_{eN}}(v_{ex}\frac{\partial v_{ez}}{\partial x} + v_{ey}\frac{\partial v_{ez}}{\partial y}) \quad (25)$$

Ambipolar Flow

No net current is assumed to flow parallel to the cathode surface in the x direction: $j_x = 0$. As a result $v_{+x} = v_{ex} = v_x$, which is easily shown from definitions (7) and (22). This is ambipolar flow, ion and electron fluids are coupled by electrostatic force and move jointly on electron thermal energy and with ion inertia.

From equation (23) it becomes evident that:

$$E_x = -\frac{D_e - D_+}{\mu_e + \mu_+} \frac{1}{n} \frac{\partial n}{\partial x} + \frac{\mu_e}{\mu_e + \mu_+} v_{ez}B_y +$$

$$-\frac{1}{\mu_e + \mu_+} \left[\frac{1}{v_{eN}}(v_{ex}\frac{\partial v_{ex}}{\partial x} + v_{ey}\frac{\partial v_{ex}}{\partial y}) - \frac{1}{v_{+N}}(v_{+x}\frac{\partial v_{+x}}{\partial x} + v_{+y}\frac{\partial v_{+x}}{\partial y}) \right] \quad (26)$$

and that equation (11) for the electric field has been reduced to:

$$\frac{\partial E_x}{\partial x} + \frac{\partial E_y}{\partial y} = 0 \quad (27)$$

Energy Equations

Ions are assumed to be cold, and their energy equation consists of a simple electrostatic acceleration along $-y$ from the distant plasma to the cathode surface. The ion energy equation will be presented at the end of this section.

The generation and flow of heat is assumed to involve only electrons. The general energy equation in Cartesian coordinates is written in indicial notation as:

$$\frac{\partial(\rho e)}{\partial t} + \frac{\partial(\rho e v_i)}{\partial x_i} + \frac{\partial q_i}{\partial x_i} + \frac{\partial(p v_i)}{\partial x_i} - \frac{\partial(v_j \sigma_{ij})}{\partial x_i} = \frac{dQ}{dt} \quad (28)$$

for quantities defined as follows:

$$e = u + \frac{v^2}{2} + \psi \quad \text{total energy per unit mass,}$$

(use of the symbol e is traditional, and as total energy will only be used until equation (29), confusion with the elementary charge in the definition of ψ , and in later sections is unlikely)

u	internal energy per unit mass
$\psi = \frac{e}{m}(\phi_\infty - \phi(\mathbf{x}))$	electric potential relative to plasma at $\mathbf{x} \rightarrow \infty$
v	speed
ρ	mass density
v_i	velocity components (subscripts $i = x, y, z$)
q_i	heat flux components
p	pressure
σ_{ij}	stress tensor
x_i	coordinates
Q	internal heat generation per unit volume.

In the interests of clarity the species subscript for the electron fluid will be suppressed until the final form of its energy equation is presented at equation (36).

A more specific electron energy equation is given from (28) by using equation (1) for electron continuity, in conjunction with the simplifying assumptions of: inviscid, $\sigma_{ij} = 0$; isothermal, $q_i = 0$; steady flow, $\partial/\partial t = 0$:

$$\rho v_i \frac{\partial e}{\partial x_i} = - \frac{\partial(pv_i)}{\partial x_i} - emS + \frac{dQ}{dt} \quad (29)$$

The electron fluid is assumed to behave as an ideal gas with constant specific heats. Thus $u = C_v T$, $p/\rho = RT$, and $C_p - C_v = R$, for a gas constant $R = k/m$, and specific heats at constant pressure and volume C_p and C_v respectively. With these assumptions, and the use of steady state continuity, equation (29) simplifies to:

$$\rho v_i \frac{\partial}{\partial x_i} \left(\frac{v^2}{2} \right) = -(C_p T + \frac{v^2}{2} + \psi)mS - \rho v_i \frac{\partial \psi}{\partial x_i} + \frac{dQ}{dt} \quad (30)$$

Potential ψ of the electron fluid is assumed to be purely electrical (e.g. no gravity), and its relationship to the voltage $\phi(\mathbf{x})$, and electric field $\mathbf{E}(\mathbf{x})$ is:

$$\nabla\psi = -\frac{e}{m}\nabla\phi = \frac{e}{m}\mathbf{E} \quad (31)$$

The plasma source function S is modeled as:

$$S(x,y) = \alpha_0 n(x,y) \quad (32)$$

where ionization coefficient α_0 is spatially uniform and highly dependent on electron temperature. Folding (31) and (32) into (30):

$$\rho \mathbf{v} \cdot \nabla \left(\frac{v^2}{2} \right) = en \left[\mathbf{v} \cdot \nabla \phi - \alpha_0 \left(C_p \frac{mT}{e} + \frac{mv^2}{2e} + \phi_\infty - \phi \right) \right] + \frac{dQ}{dt} \quad (33)$$

where e is the elementary charge.

Assuming that electron joule heating supplies all the energy needed to create plasma at the local thermal plus kinetic plus potential energy, and that there are no other internal heat sources, $dQ/dt = 0$, then each side of equation (33) equals zero so that:

$$v_x^2 + v_y^2 + v_z^2 = v_e^2 = \text{constant} \quad (34)$$

$$\mathbf{v} \cdot \nabla \phi = \alpha_0 \left(\frac{5kT}{2e} + \frac{mv^2}{2e} + \phi_\infty - \phi \right) \quad (35)$$

where $C_p = 5k/2m$.

The lateral ambipolar diffusion velocity v_x is assumed to be negligible compared to velocities along the conduction axis y , and the magnetron drift axis z . Also, E_x parallel to the cathode surface is assumed negligible compared to E_y . The final form of the electron energy equation is:

$$-E_y = \frac{\partial \phi}{\partial y} = \frac{\alpha_0}{v_{ey}} (u_e + \phi_\infty - \phi) \quad (36)$$

$$u_e \equiv \frac{5kT_e}{2e} + \frac{mv_e^2}{2e} \quad (37)$$

The ion energy equation is found by a similar development from equation (28):

$$\rho_+ \mathbf{v}_+ \cdot \nabla \left(\frac{v_+^2}{2} - \psi_+ \right) = - \left(\frac{v_+^2}{2} - \psi_+ \right) m_+ S + \frac{dQ_+}{dt} \quad (38)$$

$$\frac{v_+^2}{2} - \psi_+ = 0, \quad \frac{dQ_+}{dt} = 0 \quad (39)$$

$$v_+^2 = \frac{2e}{m_+} (\phi_\infty - \phi) \quad (40)$$

Velocity Derivatives

From velocity magnitude relationships (34) and (40), in conjunction with the assumption of $v_x = 0$, the following differentials are determined:

$$v_{+y} \frac{\partial v_{+y}}{\partial x} = \frac{eE_x}{m_+} \quad v_{+y} \frac{\partial v_{+y}}{\partial y} = \frac{eE_y}{m_+} \quad v_{ey} \partial v_{ey} = -v_{ez} \partial v_{ez} \quad (41)$$

Equation (25) for j_z simplifies as follows:

$$\frac{j_z}{en} = -\mu_e v_{ey} B_x + \frac{v_{ey}}{v_{eN}} \frac{\partial v_{ez}}{\partial y} = -v_{ez}$$

$$\frac{\partial v_{ez}}{\partial y} = v_{eN} \left(\mu_e B_x - \frac{v_{ez}}{v_{ey}} \right) \quad (42)$$

and equation (24) for j_y simplifies in the following steps:

$$\frac{j_y}{e} = n(\mu_e + \mu_+) E_y + n\mu_e v_{ez} B_x + (D_e - D_+) \frac{\partial n}{\partial y} +$$

$$- \frac{n}{v_{eN}} v_{ez} \frac{\partial v_{ez}}{\partial y} - \frac{n}{v_{+N}} \frac{e}{m_+} E_y$$

$$\begin{aligned} \frac{j_y}{en} &= (\mu_e + \mu_+)E_y + \mu_e v_{ez} B_x + \frac{D_e - D_+}{n} \frac{\partial n}{\partial y} + \\ &\quad - v_{ez} \left(\mu_e B_x - \frac{v_{ez}}{v_{ey}} \right) - \mu_+ E_y \\ \frac{j_y}{en} &= \mu_e E_y + \frac{D_e - D_+}{n} \frac{\partial n}{\partial y} + \frac{v_{ez}^2}{v_{ey}} \end{aligned} \quad (43)$$

Equation (26) for the lateral electric field E_x simplifies to:

$$E_x = - \frac{D_e - D_+}{\mu_e + \mu_+} \frac{1}{n} \frac{\partial n}{\partial x} + \frac{\mu_e}{\mu_e + \mu_+} v_{ez} B_y \quad (44)$$

Equipotentials are assumed to be purely parallel to the cathode surface, $\phi(y)$, and $E_x = 0$. This assumption is supported by Langmuir probe data.⁹ As a result:

$$v_{ez} = \frac{D_e - D_+}{\mu_e B_y} \frac{1}{n} \frac{\partial n}{\partial x} \quad (45)$$

Electron Velocities

The electron velocity components v_{ey} and v_{ez} are now determined. By subtracting electron continuity from ion continuity, equations (16), the following relationship is achieved:

$$\frac{\partial v_{+y}}{\partial y} - \frac{\partial v_{ey}}{\partial y} + \frac{v_{+y} - v_{ey}}{n} \frac{\partial n}{\partial y} = 0 \quad (46)$$

By substituting from (41) for the derivative of v_{ey} , and from ion continuity

$$\frac{\partial n}{\partial y} = \frac{n}{v_{+y}} \left(\alpha_0 - \frac{\partial v_{+y}}{\partial y} \right)$$

then (46) involves only velocities and their derivatives:

$$\left(\frac{v_{ey}}{v_{+y}}\right) \frac{\partial v_{+y}}{\partial y} + \left(\frac{v_{ez}}{v_{ey}}\right) \frac{\partial v_{ez}}{\partial y} + \left(1 - \frac{v_{ey}}{v_{+y}}\right) \alpha_0 = 0 \quad (47)$$

By employing the relationship for E_y from (41), and substituting for the derivative of v_{+y} from (47):

$$E_y = \frac{m_+}{e} \frac{v_{+y}^2}{v_{ey}} \left[\alpha_0 \left(\frac{v_{ey}}{v_{+y}} - 1 \right) - \frac{v_{ez}}{v_{ey}} \frac{\partial v_{ez}}{\partial y} \right] \quad (48)$$

By substituting ϕ for E_y by equation (31), using the negative root of (40) for v_{+y} , and using (42) for the derivative of v_{ez} , equation (48) becomes:

$$\frac{-1}{2(\phi_\infty - \phi)} \frac{d\phi}{dy} + \frac{\alpha_0}{\sqrt{\frac{2e}{m_+}(\phi_\infty - \phi)}} = \frac{-1}{v_{ey}} \left[\alpha_0 + v_{eN} \frac{v_{ez}}{v_{ey}} (\mu_e B_x - \frac{v_{ez}}{v_{ey}}) \right] \quad (49)$$

The left hand side of (49) only depends on coordinate y , therefore the right hand side must either be a function of y only, or a constant.

The ratio $\xi = v_{ez}/v_{ey}$ is found in an approximate manner by setting the $\partial/\partial x$ of the right hand side of (49) to zero, and assuming the ratio α_0/v_{eN} is small. In conjunction with (34) the results for these velocity components are:

$$\frac{v_{ez}}{v_{ey}} = \mu_e B_x \quad v_{ey} = \frac{v_e}{\sqrt{1 + \mu_e^2 B_x^2}} \quad v_{ez} = \frac{v_e \mu_e B_x}{\sqrt{1 + \mu_e^2 B_x^2}} \quad (50)$$

Note that:
$$\sqrt{1 + \mu_e^2 B_x^2} = \sqrt{1 + \frac{\omega_{cex}^2}{v_{eN}^2}}$$

where ω_{cex} is the electron cyclotron frequency based on B_x .

Potential Profile

Velocity components v_{ey} and v_{ez} vary negligibly with x in the region along the y axis where plasma is concentrated and B_x is the

major magnetic field component. A potential profile is derived from electron energy equation (36), now approximated as follows:

$$-E_y(y) = \frac{d\phi(y)}{dy} = \frac{\alpha_0}{v_{ey}(0,y)}(u_e + \phi_\infty - \phi(y)) \quad (51)$$

This is integrated to:

$$\phi(y) = (u_e + \phi_\infty)F(y)$$

$$\frac{d\phi}{dy} = \frac{\alpha_0(u_e + \phi_\infty)}{v_{ey}(0,y)}(1 - F(y))$$

$$F(y) = \int_0^y \frac{\alpha_0}{v_{ey}(0,\eta)} e^{\int_y^\eta \frac{\alpha_0}{v_{ey}(0,\xi)} d\xi} d\eta \quad (52)$$

Define distance y_∞ as the location where $\phi(y_\infty) = \phi_\infty$, and beyond which plasma is unmagnetized. Determine y_∞ by the criteria:

$$\mu_e B_x(0, y_\infty) = 1 \quad (53)$$

By equation (50), $v_{ey}(0, y_\infty) = v_e/\sqrt{2}$, and from (51) and (52):

$$-E_y(y_\infty) = \frac{\sqrt{2}\alpha_0 u_e}{v_e} = \frac{\sqrt{2}\alpha_0}{v_e}(u_e + \phi_\infty)(1 - F(y_\infty))$$

which leads to the expression for the plasma potential at y_∞ :

$$\phi_\infty = u_e \left(\frac{1}{1 - F(y_\infty)} - 1 \right) \quad (54)$$

The potential profile will be completely known once the electron drift velocity, v_e , is determined.

Electron Drift Velocity

At $y \rightarrow \infty$, uniform unmagnetized plasma has $\frac{\partial n}{\partial y} \rightarrow 0$, $v_{ez} \rightarrow 0$, and equation (43) for j_y collapses to $j_y \rightarrow j_\infty = -en_\infty v_e = en_\infty \mu_e E_{y\infty}$. Here v_e is the constant electron drift velocity conveying the circuit current between the anode and the magnetron region, and $E_{y\infty}$ is the constant electric field in this positive column. From (51) for E_y it is evident that:

$$E_{y\infty} = -\frac{v_e}{\mu_e} = \frac{j_\infty}{en_\infty \mu_e} = -\frac{\alpha_0 u_e}{v_e} = -\frac{\alpha_0}{v_e} \left(\frac{5kT_e}{2e} + \frac{m_e v_e^2}{2e} \right) \quad (55)$$

Solving (55) for v_e produces:

$$v_e^2 = \frac{\frac{5kT_e}{m_e}}{\frac{2v_{eN}}{\alpha_0} - 1} = \left(\frac{j_\infty}{en_\infty} \right)^2 \quad (56)$$

Independent parameters are seen to be T_e , v_{eN} , α_0 , and either j_∞ or n_∞ (both v_{eN} and α_0 depend on T_e as well as gas molecule properties).

At this point both $\phi(y)$ and $E_y(y)$ are considered known. Since $E_z = E_x = 0$, and $\nabla \cdot \mathbf{E} = 0$, then an exact solution requires $\frac{dE_y}{dy} = 0$. This condition is not met, the disparity being greatest at the cathode surface and diminishing to insignificance at $y \rightarrow \infty$. This discrepancy is a consequence of the absence of electrostatic sheaths in this model.

Plasma Density Profile

Equating expressions (45) and (50) for v_{ez} yields an expression for plasma density:

$$\frac{1}{n} \frac{\partial n}{\partial x} = \frac{v_e}{D_e - D_+} \frac{\mu_e^2 B_x B_y}{\sqrt{1 + \mu_e^2 B_x^2}} \quad (57)$$

This is integrated along x at constant y between coordinates $-x_p$ and $+x_p$ which are centered on the magnets flanking the magnetron track:

$$n(x,y) = n(-x_p,y) \exp \left[\frac{v_e}{D_e - D_+} \int_{-x_p}^x \frac{\mu_e^2 B_x B_y}{\sqrt{1 + \mu_e^2 B_x^2}} dx \right] \quad (58)$$

Given $n(-x_p,y)$, the density profile above the magnet pole, then $n(x,y)$ is determined. Note that the choice of magnet centers $\pm x_p$ as the lateral limits of investigation is arbitrary and simply a matter of convenience. Equation (58) is relabeled to simplify later algebra:

$$n(x,y) = n_0(y) L(x,y) \quad n_0(y) \equiv n(-x_p,y) \quad (59)$$

and $L(x,y)$ is the exponential function in (58). From (59):

$$\frac{\partial n}{\partial y} = L \frac{\partial n_0}{\partial y} + n_0 \frac{\partial L}{\partial y} \quad (60)$$

Equation (43) for j_y is now revisited and expressions (59) and (60) are introduced:

$$j_y = en_0 L \mu_e E_y + e(D_e - D_+) \left[L \frac{dn_0}{dy} + n_0 \frac{\partial L}{\partial y} \right] + en_0 L \frac{v_{ez}^2}{v_{ey}}$$

$$j_y = en_0 \left[L (\mu_e E_y + \frac{v_{ez}^2}{v_{ey}}) + (D_e - D_+) \frac{\partial L}{\partial y} \right] + e(D_e - D_+) L \frac{dn_0}{dy} \quad (61)$$

The conservation of the circuit current I_0 is given by an area integral of equation (61) for j_y , and this provides an expression for the determination of $n_0(y)$:

$$I_0 \equiv \int_z \int_{-x_p}^{+x_p} j_y dx dz = \Delta z \int_{-x_p}^{+x_p} j_y dx = \Delta z 2x_p j_{\infty} \quad (62)$$

$$I_0 = b(y)n_0 + a(y) \frac{dn_0}{dy} \quad (63)$$

$$a(y) \equiv \Delta z e (D_e - D_+) \int_{-x_p}^{+x_p} L(x,y) dx \quad (64)$$

$$b(y) \equiv \Delta z e \int_{-x_p}^{+x_p} \left[L \cdot \left(\mu_e E_y + \frac{v_{ez}^2}{v_{ey}} \right) + (D_e - D_+) \frac{\partial L}{\partial y} \right] dx \quad (65)$$

and Δz is the length of the magnetron track which intercepts total circuit current I_0 . Equation (63) is integrated for $n_0(y)$, and for convenience these functions are defined:

$$H(y) \equiv b(y)/a(y) \quad K(y) \equiv I_0/a(y) \quad (66)$$

Note from $K(y)$ that circuit current per unit magnetron track length, $I_0/\Delta z$, enters as a parameter to $n(x,y)$ rather than any absolute current or track length. The final form of $n_0(y)$ is:

$$n_0(y) = e^{-\int_0^y H(\eta) d\eta} \cdot [n_0(0) + \int_0^y K(\eta) \cdot e^{\int_0^\eta H(\xi) d\xi} d\eta]$$

$$n_0(0) = n_\infty e^{\int_0^{y_\infty} H(\eta) d\eta} - \int_0^{y_\infty} K(\eta) \cdot e^{\int_0^\eta H(\xi) d\xi} d\eta \quad (67)$$

and $n(x,y) = n_0(y)L(x,y)$ for $L(x,y)$ as defined by (58) and (59), and $n_0(y)$ as given by (67). Also note that for positive current in the $-y$ direction that I_0 , j_∞ , and K are negative.

Magnetron Current

The magnetron current along $-z$ is:

$$I_M = \int_0^{y_\infty} \int_{-x_p}^{+x_p} -e n(x,y) v_{ez}(x,y) dx dy \quad (68)$$

Summary of Analytical Results:

$$v_e^2 = \frac{5kT_e}{\frac{m_e}{2\frac{v_e N}{\alpha_0} - 1}} = \left(\frac{j_\infty}{en_\infty}\right)^2 \quad (56)$$

$$\frac{v_{ez}}{v_{ey}} = \mu_e B_x \quad v_{ey} = \frac{v_e}{\sqrt{1 + \mu_e^2 B_x^2}} \quad v_{ez} = \frac{v_e \mu_e B_x}{\sqrt{1 + \mu_e^2 B_x^2}} \quad (50)$$

$$\mu_e B_x(0, y_\infty) = 1 \quad (53)$$

$$F(y) = \int_0^y \frac{\alpha_0}{v_{ey}(0, \eta)} e^{\int_y^\eta \frac{\alpha_0}{v_{ey}(0, \xi)} d\xi} d\eta \quad (52)$$

$$u_e \equiv \frac{5kT_e}{2e} + \frac{mv_e^2}{2e} \quad (37)$$

$$\phi_\infty = u_e \left(\frac{1}{1 - F(y_\infty)} - 1 \right) \quad (54)$$

$$\phi(y) = (u_e + \phi_\infty) F(y) \quad (52)$$

$$\frac{d\phi}{dy} = \frac{\alpha_0(u_e + \phi_\infty)}{v_{ey}(0, y)} (1 - F(y)) = -E_y \quad (52)$$

$$v_+^2 = \frac{2e}{m_+} (\phi_\infty - \phi) \quad (40)$$

$$n(x, y) \equiv n_0(y) L(x, y) \quad n_0(y) \equiv n(-x_p, y) \quad (59)$$

$$n(x, y) = n(-x_p, y) \exp \left[\frac{v_e}{D_e - D_+} \int_{-x_p}^x \frac{\mu_e^2 B_x B_y}{\sqrt{1 + \mu_e^2 B_x^2}} dx \right] \quad (58)$$

$$a(y) \equiv \Delta z e (D_e - D_+) \int_{-x_p}^{+x_p} L(x,y) dx \quad (64)$$

$$b(y) \equiv \Delta z e \int_{-x_p}^{+x_p} \left[L \cdot \left(\mu_e E_y + \frac{v_{ez}^2}{v_{ey}} \right) + (D_e - D_+) \frac{\partial L}{\partial y} \right] dx \quad (65)$$

$$H(y) \equiv b(y)/a(y) \quad K(y) \equiv I_0/a(y) \quad (66)$$

$$n_0(0) = n_\infty e^{\int_0^{y_\infty} H(\eta) d\eta} - \int_0^{y_\infty} K(\eta) \cdot e^{\int_0^\eta H(\xi) d\xi} d\eta \quad (67)$$

$$n_0(y) = e^{-\int_0^y H(\eta) d\eta} \cdot \left[n_0(0) + \int_0^y K(\eta) \cdot e^{\int_0^\eta H(\xi) d\xi} d\eta \right] \quad (67)$$

$$I_M = \int_0^{y_\infty} \int_{-x_p}^{+x_p} -e n(x,y) v_{ez}(x,y) dx dy \quad (68)$$

An Example

Application of the model is illustrated with the following example drawn from experimental results published by Wendt and Lieberman.⁵ A circular planar magnetron with $B_x(0,0) = 171$ Gauss in a 5 cm wide, 31.4 cm long track, intercepts 0.5 Amps of discharge current at 520 Volts in 5 mTorr of argon. Measurements of the current density $j_y(x,0)$ at the cathode surface are fitted by a gaussian in coordinate x with a FWHM of 1.875 cm and a peak of 0.14 A/cm².

An example was calculated for $p = 5$ mTorr ($N = 1.77 \times 10^{14}$ cm⁻³), argon ($Z = 39.948$ AMU ions), $I_0/\Delta z = -1.59$ Amp/m ($= -0.5$ A/0.314 m), with $B_x(0,0) = 178$ Gauss. Parameters were selected as follows: $T_e = 5$ eV, $v_{eN} = 1.24 \times 10^7$ s⁻¹, $\alpha_0 = 7.09 \times 10^4$ s⁻¹, $j_\infty = -0.00318$ A/cm². The diffusion and mobility coefficients used were: $D_e = 7.08 \times 10^4$ m²/s, $D_+ = 41.4$ m²/s,

$\mu_e = 1.42 \times 10^4 \text{ m}^2/\text{s-Volt}$, $\mu_+ = 331 \text{ m}^2/\text{s-Volt}$.

Results are: $n_\infty = 1.77 \times 10^9 \text{ cm}^{-3}$, $v_e = 1.12 \times 10^7 \text{ cm/s}$,
 $y_\infty = 22.4 \text{ cm}$, $u_e = 12.5 \text{ eV}$, $\phi_\infty = 522 \text{ Volts}$, $I_M = -0.773 \text{ A}$, $I_M/I_0 = 1.55$,
 $n(0,0) = 2.28 \times 10^{11} \text{ cm}^{-3}$, $j_y(0,0) = -0.185 \text{ A/cm}^2$.

Figures 3, 4, 5, 6, 7, and 8 show spatial distributions as one of:
1) graphs along x between $-x_p$ and $+x_p$ at the cathode surface ($y = 0$),
2) surface plots for $-x_p \leq x \leq +x_p$, $y \leq y_\infty$, oriented as is Figure 2, and
3) graphs along y from 0 to y_∞ , at mid-track ($x = 0$).

Parameter Studies

The value of an accurate fluid model would be the ability to design magnetron cathodes with desired attributes, by specifying both the magnet strength and geometry, and the gas properties. A magnetron cathode could be designed for a higher sputtering yield at lower voltage by narrowing the density distribution, or a broad density distribution could be selected for a uniform erosion pattern and long cathode life. An example of a broad density distribution is shown in Figure 2.

A sample parameter study is the calculation of ϕ_∞ where the only parameter varied is the angle of tilt, θ , of the magnets flanking the magnetron track. This angle is defined as positive for outward tilt, and negative for inward tilt. Figure 1 shows magnetron tracks with one side tilted inward -15° .

These calculations model a single 2 cm wide track like that on the left in Figure 1, but with both magnets tilted with mirror symmetry. Conditions are: a 35 mTorr mixture of 1% O_2 in helium, $T_e = 6 \text{ eV}$ (He^+ and O^+ in equal numbers), $I_0/\Delta z = -2000 \text{ A/m}$, $B_x(0,0) = 840 \text{ Gauss}$ at $\theta = 0^\circ$. Calculations show that ϕ_∞ decreases with inward tilt, and increases to a maximum then decreases with outward tilt. The influence of θ on voltage is shown in Figure 9. Experiments are being planned to verify this model.

This work was performed under the auspices of the U.S. DOE by LLNL under contract no. W-7405-Eng-48.

References

- 1) R. K. Waits, "Planar magnetron sputtering," *Journal of Vacuum Science Technology*, Volume 15, Number 2, March/April 1978, pps. 179-187.
- 2) S. M. Rossnagel, "Induced drift currents in circular planar magnetrons," *Journal of Vacuum Science Technology A*, Volume 5, Number 1, Jan./Feb. 1987, pps. 68-91.
- 3) S. M. Rossnagel, H. R. Kaufman, "Current-voltage relations in magnetrons," *Journal of Vacuum Science Technology A*, Volume 6, Number 2, March/April 1988, pps. 223-229.
- 4) L. McCaig, R. Sacks, D. Lubman, "Radiative and Electrical Properties of a Planar Magnetron Glow Discharge Device," *Applied Spectroscopy*, Volume 43, Number 6, 1989, pps 912-917.
- 5) A. E. Wendt, M. A. Lieberman, "Spatial structure of a planar magnetron discharge," *Journal of Vacuum Science Technology A*, Volume 8, Number 2, March/April 1990, pps. 902-907.
- 6) T. E. Sheridan, M. J. Goeckner, J. Goree, "Electron and ion transport in magnetron plasmas," *Journal of Vacuum Science Technology A*, Volume 8, Number 3, May/June 1990, pps. 1623-1626.
- 7) M. D. Bowden, T. Nakamura, K. Muraoka, Y. Yamagata, B. W. James, M. Maeda, "Measurement of the cathode sheath in a magnetron sputtering discharge using laser induced fluorescence," *Journal of Applied Physics* Volume 73, Number 8, 15 April 1993, pps. 3664-3667.
- 8) B. W. Manley, "Planar Magnetron Sputtering Magnet Assembly," *United States Patent*, Number 5,262,028, November 16, 1993.
- 9) P. Spatenka, I. Leipner, J. Vlcek, J. Musil, "Langmuir probe measurements of plasma parameters in a planar magnetron with additional plasma confinement," *Proceedings of the 12th International Symposium on Plasma Chemistry*, Volume 1, pps 487-492. A wider variety of data was shown at the symposium than in the published paper.

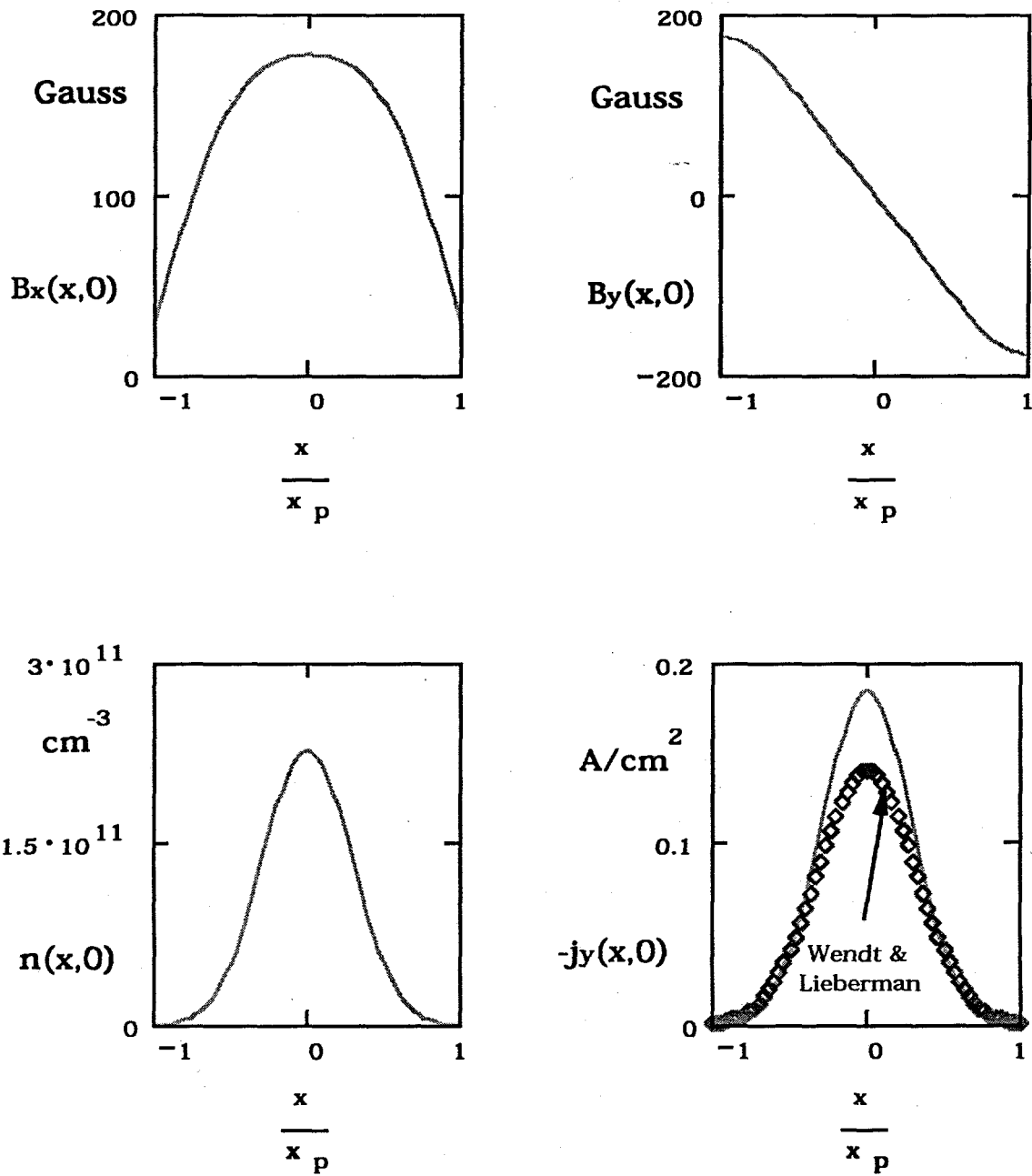
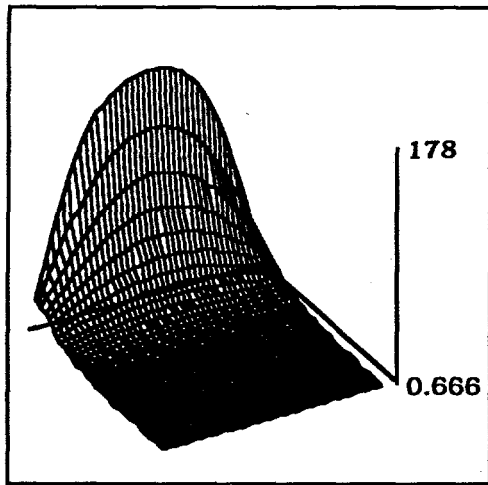
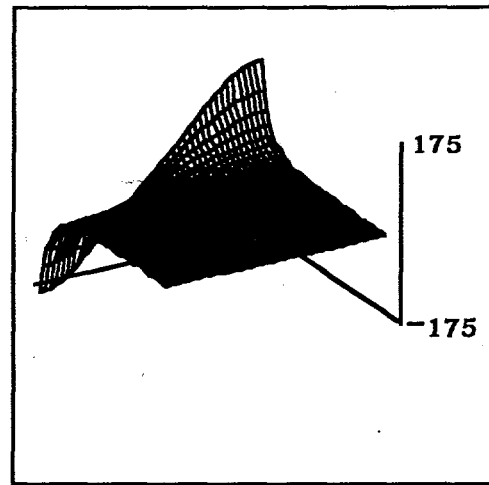


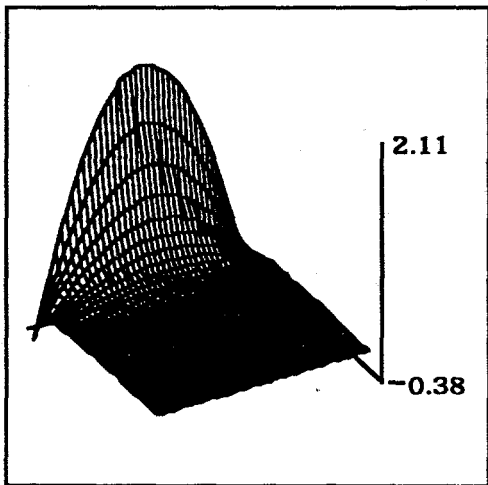
Figure 3: Surface distributions across magnetron track B_x , B_y , n , and j_y at $y = 0$, and j_y from experiment in reference [5]



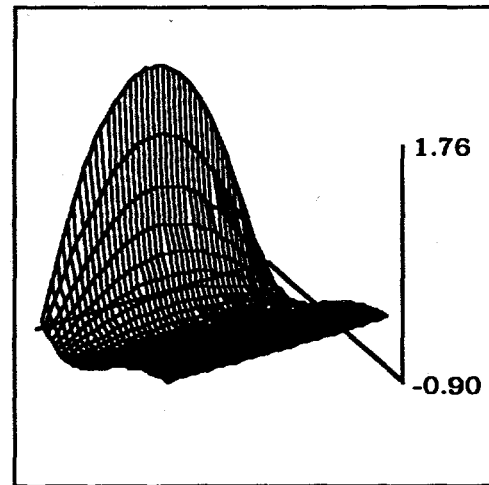
B_x , Gauss



B_y , Gauss

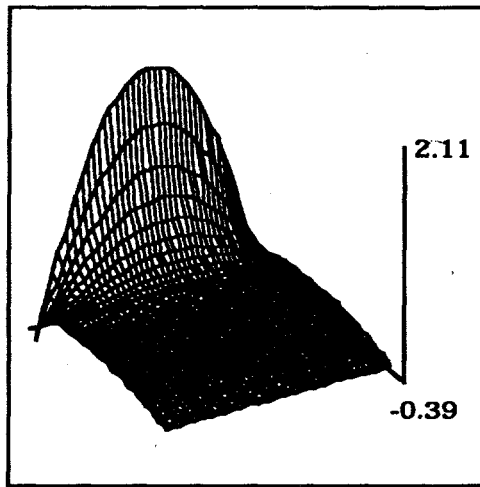


$\text{Log} [n(x,y)/n_\infty]$

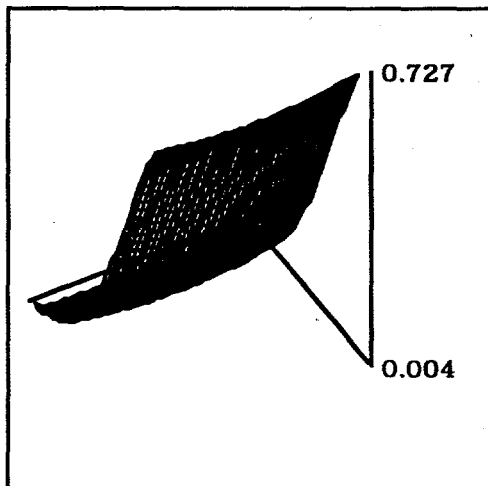


$\text{Log} [j_y(x,y)/j_\infty]$

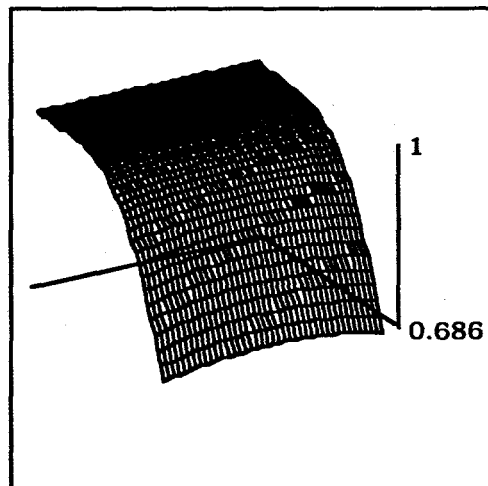
Figure 4: Distribution of B , n , and j_y between $\pm x_p$ and y_∞ . These surface plots are oriented exactly as Figure 2.



$\text{Log} [j_z(x,y)/j_\infty]$



$v_{ey}(x,y)/v_e$



$v_{ez}(x,y)/v_e$

Figure 5: Distribution of j_z , v_{ey} , and v_{ez} between $\pm x_p$ and y_∞ . These surface plots are oriented exactly as Figure 2

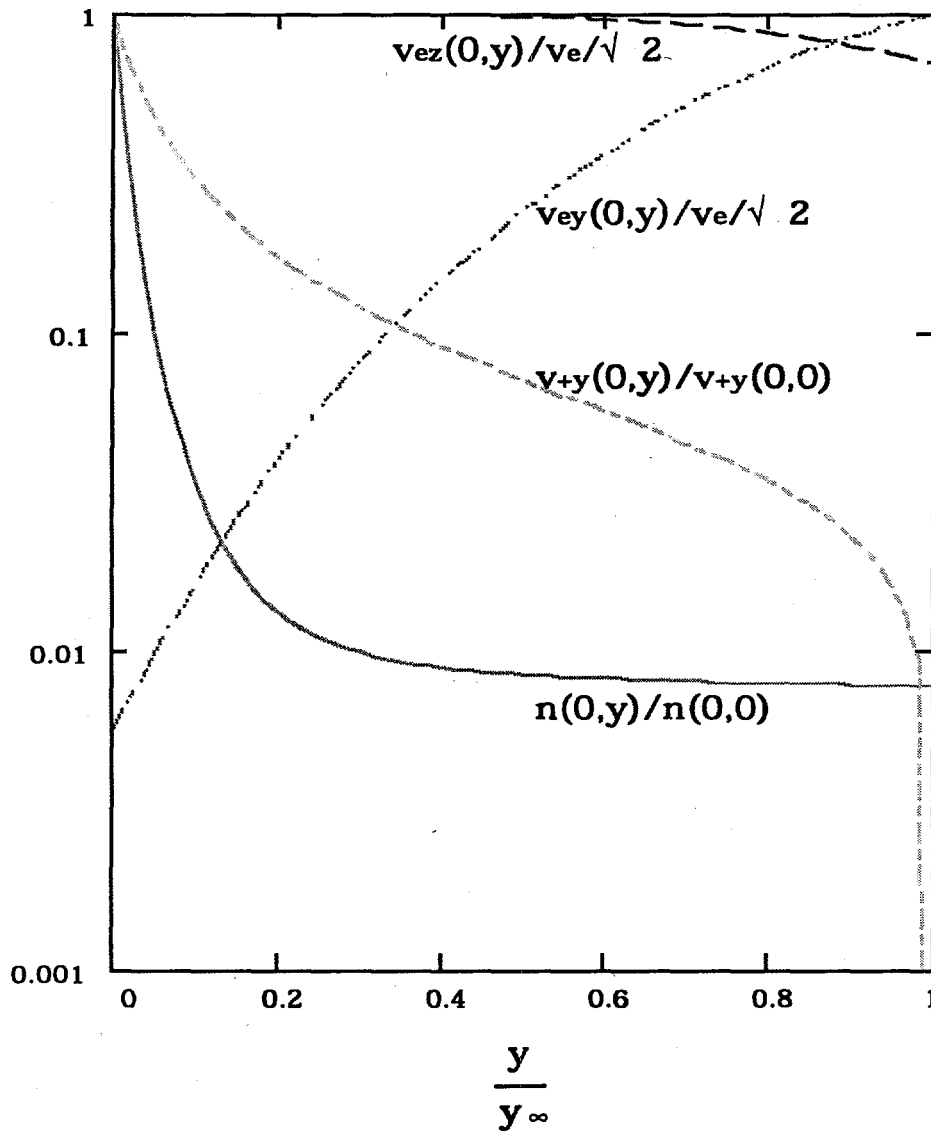


Figure 6: Normalized density and velocities at mid-track Profiles of v_{ez} , v_{ey} , v_{+y} , and n , along conduction axis at $x = 0$

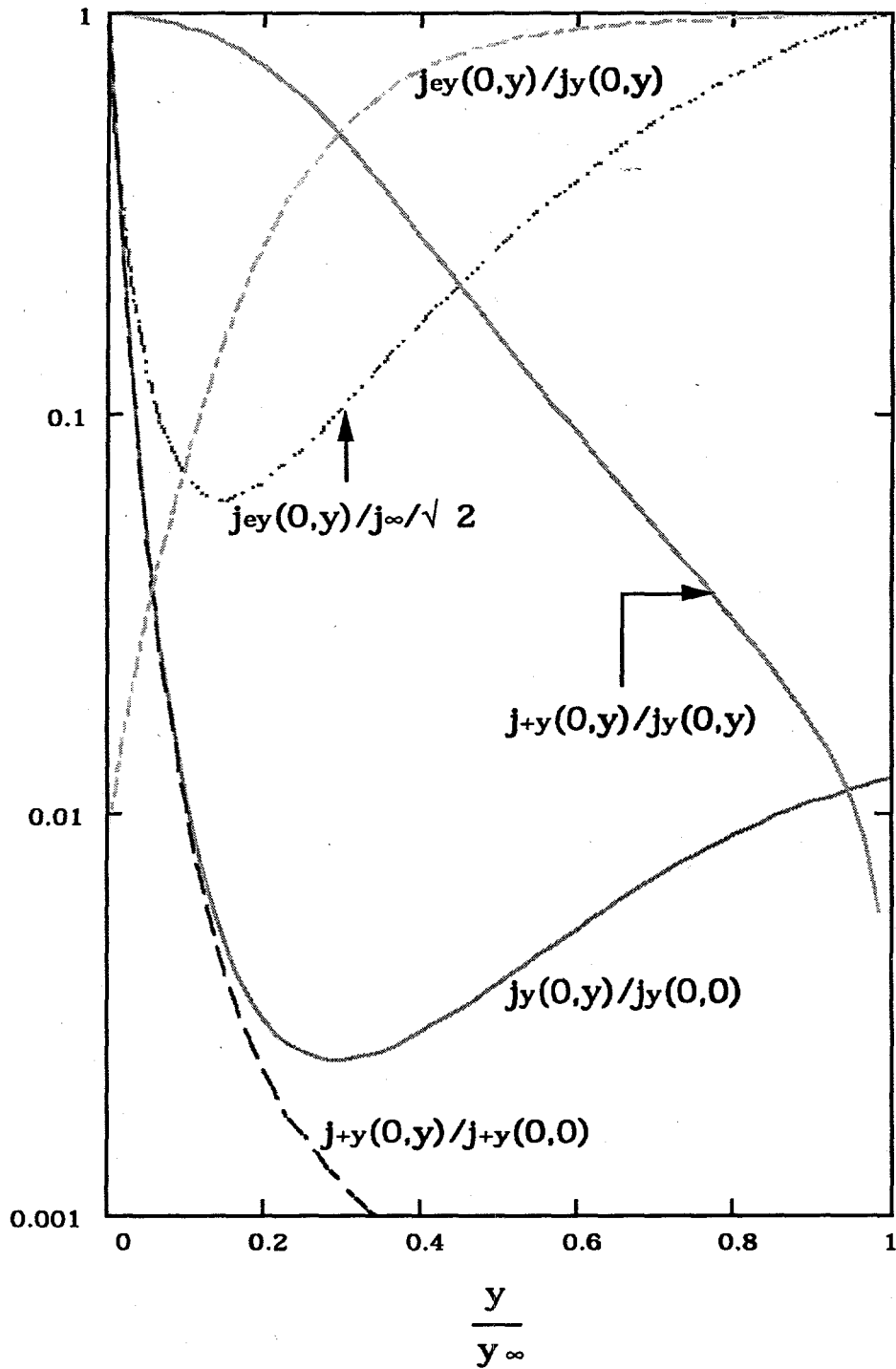


Figure 7: Normalized current densities at mid-track
 Various profiles of j_{ey} , j_{+y} , and j_y along the conduction axis at $x = 0$

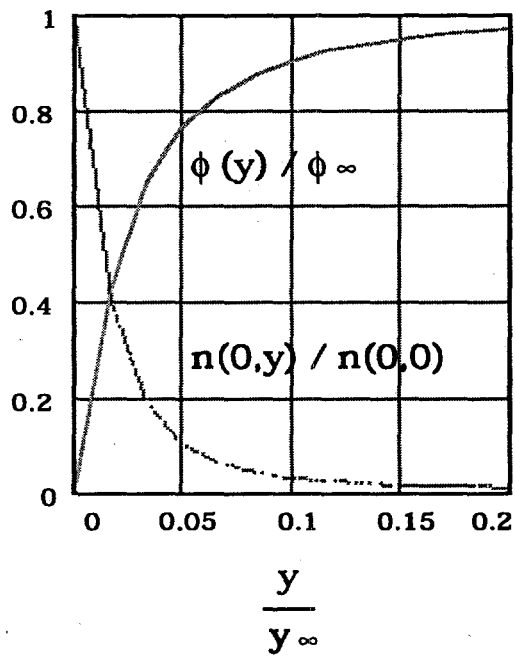
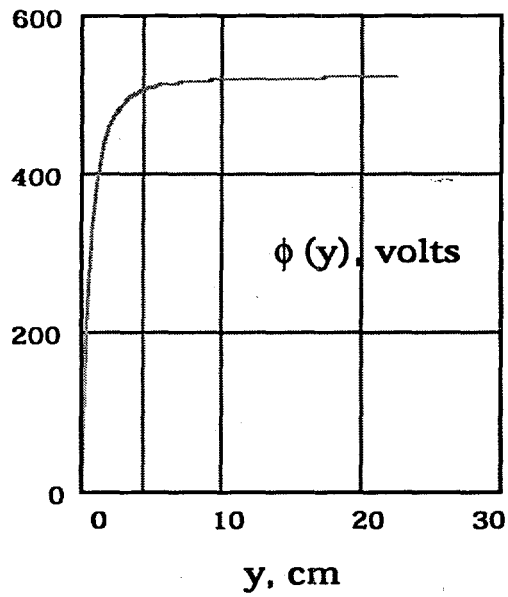


Figure 8: Voltage and density profiles at mid-track ($x = 0$)

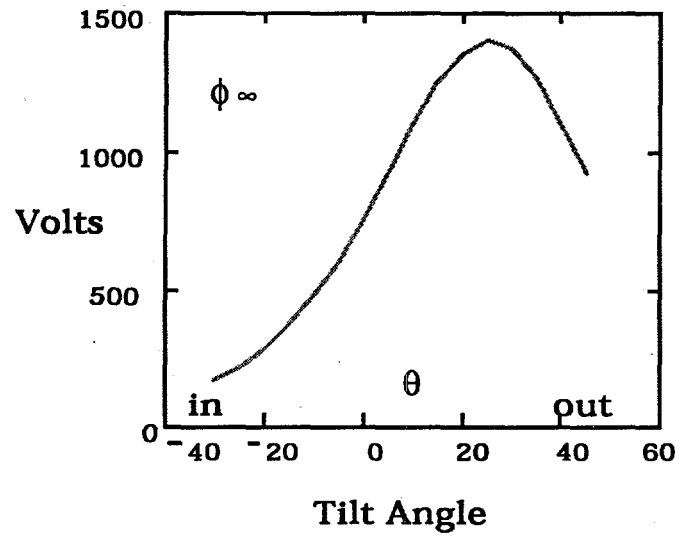


Figure 9: Effect of magnet tilt angle on voltage
 $p = 35$ mTorr, He/O₂ = 0.99/0.01, $x_p = 0.95$ cm,
 $B_x(0,0) = 840$ Gauss @ $\theta = 0^\circ$, $I_0/\Delta z = -2000$ A/m, $T_e = 6$ eV